Giant enhancement of second harmonic generation in a finite photonic crystal with a single defect and dual-localized modes

Fang-Fang Ren, Rui Li, Chen Cheng, and Hui-Tian Wang*
National Laboratory of Solid State Microstructures and Department of Physics, Nanjing University, Nanjing 210093, China

Jianrong Qiu and Jinhai Si
Photon Craft Project, Japan Science and Technology Corporation, Keihanna-Plaza, Kyoto 619-0237, Japan

Kazuyuki Hirao
Graduate School of Engineering, Kyoto University, Kyoto 606-8501, Japan
(Received 10 May 2004; revised manuscript received 12 August 2004; published 9 December 2004)

We present a one-dimensional defective photonic crystal containing the nonlinear medium, with a single defect and dual-localized modes. Giant enhancement of second harmonic generation is predicted in numerical simulation. The mechanism is the strong localizations of fundamental wave and second harmonic in the single defect, simultaneously. Such a kind of structures can be expected as high-efficency nonlinear photonic devices.

DOI: 10.1103/PhysRevB.70.245109 PACS number(s): 42.70.Qs, 42.65.Ky, 42.25.Bs

Photonic crystals (PC's)[1,2] have opened up a subject as a new kind of microstructure material. The nature of PC's is the existence of a photonic band gap (PBG), i.e., a range of frequencies, in which electromagnetic wave propagation is forbidden. PC's have attracted considerable interest because of the access to many new effects in fundamental physics and potential applications. Some efforts toward nonlinear processes such as second harmonic generation (SHG) were focused on the finite yet perfect PC's.[3–9] If the perfect structure is frustrated in the appropriate manner, that is to say, suitable defects are introduced, the resulting some allowed states within the PBG can give rise to the field enhancement in the defects. If the nonlinearity is also introduced to the defective PC's simultaneously, which may be of great importance, because they can achieve numerous functional photonic devices based on many new properties. The enhanced nonlinearities, caused by the remarkable capabilities of localizing electromagnetic wave, suggest the impressive opportunity for achieving compact yet high-efficiency photonic devices. Despite the some amount of research on the nonlinearly defective PC's,[10–13] whether the nonlinear phenomena have still not attention enough. In principle, in the cases discussed in Refs. 10 and 11, the harmonic efficiencies could not be high enough; because the SHG originates from only the nonlinear interaction of interfaces between layers, whereas the nature of strong localization was not availably exploited. Shi *et al.*[12] demonstrated the great enhancement of SHG in the defective PC's, and Dolgova *et al.*[13] verified the enhancement of SHG in PC's with single and coupled microcavities (defects); both are attributed to the mechanism of the resonant fundamental field and wave coupling caused by light localization in defect states. In a recent article[14] a review regarding enhancement of nonlinear effects in PC's can be found. In the present work, we designed a defective PC, in which the introducing of a single defect gives rise to the dual-localized modes (states) at the fundamental wave (FW) and second harmonic (SH), where the distinctive benefit of defective PC's is of most use. Numerical results by the shooting method[15] indicate the giant enhancement of SHG in such a defective PC.

For simplicity, we choose a one-dimensional structure as an example. The matrix of the constructed defective PC is a finite perfect periodic PC, as shown in Fig. 1(a). It is composed of alternately stacked *N*-*L* layers surrounded with *L* medium, where *N* and *L* indicate the nonlinear and linear layers. $LiNbO_3$ crystal is chosen as the nonlinear material. From the temperature dependent dispersion of $LiNbO_3$,[16] the parameters of the designed perfect PC are as follows: thicknesses and refractive indices of the *N* and *L* and layers are $l_N=304$ nm and $l_L=351$ nm, n_N (=2.157 at $\lambda_{FW}=1064$ nm and =2.237 at $\lambda_{SH}=532$ nm at a temperature of 150 °C), and $n_L=1.0$ (air), respectively. We change the thickness of the central *N* layer from l_N to $l_D=737$ nm, to introduce a defect, as shown in Fig. 1(b). Such a defective PC exhibits mirror-symmetry with respect to the the defect layer (the left and right sides of the defect layer have the same periods *PN*). There are two kinds of gratings: the linear grating $\epsilon(x)$ or $n(x)$ and the quadratic nonlinear grating $\chi^{(2)}(x)$ or $d(x)$.

Before investigating the SHG problem, we first discuss some linear behaviors caused by the linear grating. Such a defective PC can be equivalent to a F-P cavity,[17] as shown in Fig. 1(c). The left and right sides (containing the interfaces)

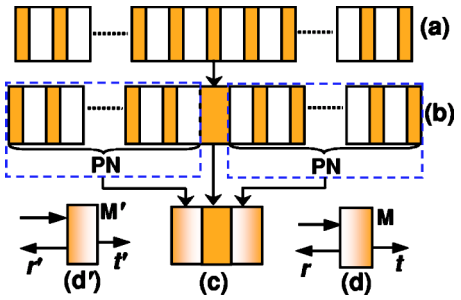

FIG. 1. (Color online) Geometric structure of PC. (a) Perfect periodic PC, (b) defective PC, (c) equivalent F-P cavity structure of defective PC, (d) and (d′) equivalent mirrors.

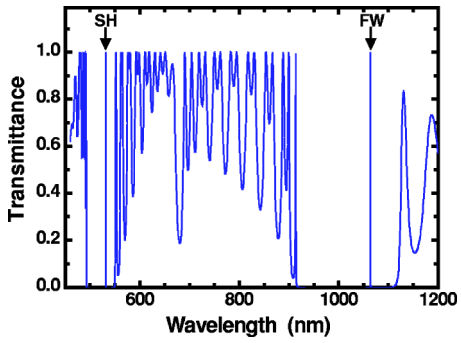

FIG. 2. (Color online) Transmission spectrum of the defective PC.

of the defect are considered as two mirrors M' and M, respectively, as seen in Figs. 1(d′) and 1(d). M' and M can be described by transfer matrices $\boldsymbol{M}'$ and $\boldsymbol{M}$, respectively. On the basis of the transfer-matrix method,[18] we give $\boldsymbol{M}' = (\boldsymbol{M}_{LN}\boldsymbol{M}_N\boldsymbol{M}_{NL}\boldsymbol{M}_L)^{PN}\boldsymbol{M}_{LN}$ and $\boldsymbol{M} = \boldsymbol{M}_{NL}(\boldsymbol{M}_L\boldsymbol{M}_{LN}\boldsymbol{M}_N\boldsymbol{M}_{NL})^{PN}$. $\boldsymbol{M}_{LN(NL)}$ is the transfer matrix in the L-N(N-L) interface and $\boldsymbol{M}_{L(N)}$ is the propagation matrix in the L(N) layer, respectively. They are

$$\boldsymbol{M}_{LN(NL)} = \frac{1}{t_{LN(NL)}}\begin{bmatrix} 1 & r_{LN(NL)} \\ r_{LN(NL)} & 1 \end{bmatrix}, \tag{1}$$

$$\boldsymbol{M}_{L(N)} = \begin{bmatrix} \exp[-jkn_{L(N)}l_{L(N)}] & 0 \\ 0 & \exp[jkn_{L(N)}l_{L(N)}] \end{bmatrix}, \tag{2}$$

where $k = 2\pi/\lambda$, and $r_{LN(NL)}$ and $t_{LN(NL)}$ are the Fresnel reflection and transmission coefficients in the L-N(N-L) interface. If $\boldsymbol{M}'$ and $\boldsymbol{M}$ are written as

$$\boldsymbol{M}' = \begin{bmatrix} a' & b' \\ c' & d' \end{bmatrix}, \boldsymbol{M} = \begin{bmatrix} a & b \\ c & d \end{bmatrix}, \tag{3}$$

the complex amplitude reflection (transmission) coefficients of M' and M could be given by $r' = c'a'^{-1}(t' = a'^{-1})$ and $r = ca^{-1}(t = a^{-1})$, respectively.

The total transfer matrix of the whole defective PC should be $\boldsymbol{M}_{\text{total}} = \boldsymbol{M}'\boldsymbol{M}_D\boldsymbol{M}$, where $\boldsymbol{M}_D$ is the propagation matrix in the defect layer and has the same form as Eq. (2) provided that l_N is replaced by l_D. $\boldsymbol{M}_{\text{total}}$ is also written as

$$\boldsymbol{M}_{\text{total}} = \begin{bmatrix} A & B \\ C & D \end{bmatrix}. \tag{4}$$

Thus the transmittance T_{total} can be calculated by $T_{\text{total}} = |A^{-1}|^2$. The transmission spectrum in Fig. 2 shows that there occurs two sharp peaks at λ_{FW} and λ_{SH} within two discrete PBG's, respectively. The spatial distributions of relative amplitudes in Fig. 3 indicate that greatly enhanced light fields at λ_{FW} and λ_{SH} are mightily localized spatially near the defect.

The introduction of the equivalent F-P cavity concept is available for understanding the localization properties in the defective PC's. The transmittance of the defective PC and the relative field distribution inside the defect can be easily yielded[17]

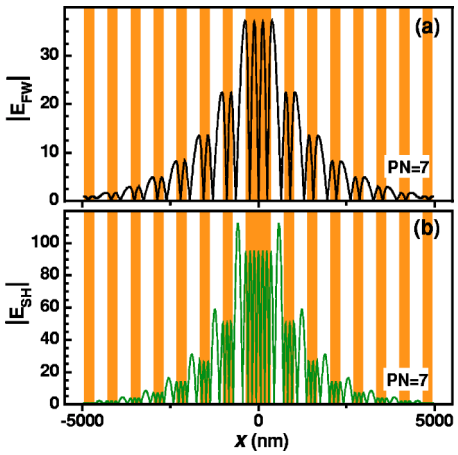

FIG. 3. (Color online) Relative amplitude distributions of FW (a) and SH (b) inside the defective PC.

$$T = \frac{1}{1 + [4r_0^2/(1 - r_0^2)^2]\sin^2\Phi}, \tag{5}$$

$$|E(x)| = |t'|\sqrt{\frac{(1 + r_0)^2 - 4r_0\sin^2(\Phi/2 - kn_Nx)}{(1 - r_0^2)^2 + 4r_0^2\sin^2\Phi}}, \tag{6}$$

where $\Phi = \phi_0 + kn_Nl_D$, x is the position coordinate $(-l_D/2 \leqslant x \leqslant l_D/2)$ in the defect, and $r = r_0\exp(i\phi_0)$. In the defective PC the phase shift ϕ_0 is no longer zero or π. We see from Eqs. (5) and (6) that alone when $\Phi = \phi_0 + kn_Nl_D = m\pi$ (m indicates the order of localized modes), the defective PC exhibits a maximum transmittance of $T = 1$ and at the same time the field in the defect is greatly enhanced; otherwise T and $|E(x)|$ fall rapidly into near zero and very low level, respectively. If $l_D = l_N$, we find from Eq. (5) that the transmittance at λ_{FW} and λ_{SH} approach zero, implying that there are no localized modes within the PBG's, because the defective PC has degenerated into a perfect periodic PC. When $l_D = 737$ nm, from Eq. (5) the two transmittance at λ_{FW} and λ_{SH} arrive at their maximum values of $T = 1$ and from Eq. (6) the FW and SH fields in the defect are greatly enhanced simultaneously. For example, for $PN = 7$, the field amplitudes $|E_{\text{FW}}|_{\max}$ and $|E_{\text{SH}}|_{\max}$ are enhanced by ~36 and ~95 multiples, respectively. These results agree completely with the results given by the transfer-matrix method (in Fig. 3). The spectral linewidths, the orders, the relative fields, and positions of the localized modes are conveniently given, based on the equivalent F-P cavity. For instance, the orders of the localized modes are the third and eighth orders for FW and SH, due to $\Phi = 3\pi$ at λ_{FW} and $\Phi = 8\pi$ at λ_{SH}. $\Delta\lambda_{\text{FW}}$ and $\Delta\lambda_{\text{SH}}$ (linewidths) as well as $|E_{\text{FW}}|_{\max}$ and $|E_{\text{SH}}|_{\max}$ as functions of PN are shown in Fig. 4. $\Delta\lambda_{\text{FW}}$ and $\Delta\lambda_{\text{SH}}$ narrow while $|E_{\text{FW}}|_{\max}$ and $|E_{\text{SH}}|_{\max}$ increase, exponentially, with increasing PN. The results confirm that a single defect can give rise to the simultaneous dual-localized modes at λ_{FW} and λ_{SH}. We predict that such dual-localization feature should cause the giant enhancement of SHG. It is of great importance that the adoption of equivalent F-P cavity can not only give the more information and the more clearly physical picture for the

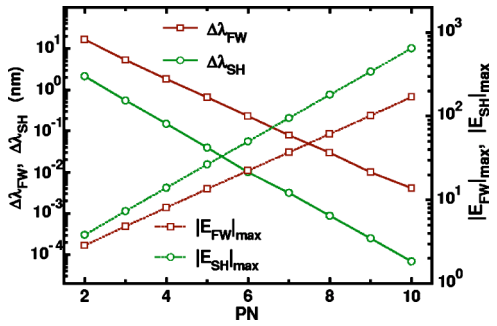

FIG. 4. (Color online) Linewidths of localized modes and maximum relative amplitudes in the defect as functions of *PN*.

localized modes but also provide a much easier and simpler means for designing the defective PC's.

In such a defective PC, we give a quantitative calculation for the total conversion efficiency of the forward and backward SH generated. The coupled-wave equations governing quadratic nonlinear interaction of two monochromatic plane waves with different wavelengths at λ_{FW} and λ_{SH} in the defective PC can be written as

$$d^2E_1/dx^2 + k_1^2 n_1^2(x)E_1 = -2k_1^2 d(x)E_1^* E_2,$$

$$d^2E_2/dx^2 + k_2^2 n_2^2(x)E_2 = -k_2^2 d(x)E_1^2. \quad (7)$$

Subscripts 1 and 2 in Eq. (7) indicate the physical quantities related with FW and SH, respectively. $n_j(x)$ and $d(x)$ is the spatial dependent refractive index and quadratic nonlinear optical coefficient, respectively. Eq. (7) can be solved numerically by the use of the shooting method,[15] which is a powerful technique for treating two-point boundary-value nonlinear problems and is unnecessary to perform the transform between the time-domain and the frequency domain. For the sake of comparison, we also choose the effective nonlinear coefficient d_{eff} of the *N* layers to be 43.9 pm/V as in Ref. 12.

We investigate in detail the dependences of the conversion efficiency on the incident FW intensity I_{0FW} and *PN*. Figure 5 shows the efficiencies as functions of I_{0FW} when $PN=7$, the squares and the circles are η_{DL} for the dual localization and η_{SL} for the single localization,[12] respectively.

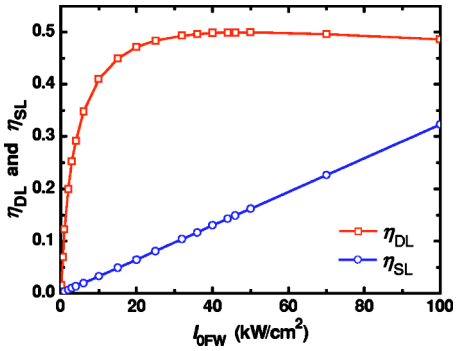

FIG. 5. (Color online) Dependence of conversion efficiency on FW intensity (for clarity η_{SL} has been magnified by a factor of 5×10^3).

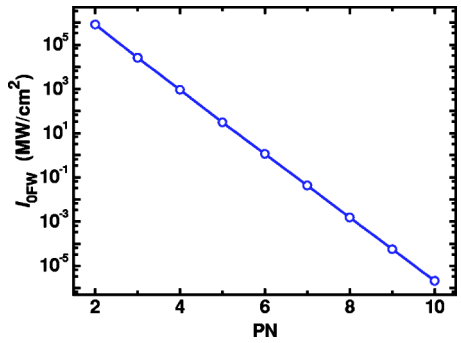

FIG. 6. (Color online) FW intensity required for 50% efficiency as a function of *PN*.

It is clear that the efficiency in the case of dual localization is about 4 orders of magnitude higher than that in the case of the single localization. For $PN=7$ and when $I_{0FW}=50$ kW/cm^2, η_{DL} can achieve 50%, whereas η_{SL} is only $\sim3\times10^{-4}$. For the film sample with the same total thickness (9.907 μm) and the same d_{eff} as the defective PC, the efficiency is only $\sim10^{-8}$ at $I_{0FW}=50$ kW/cm^2, which is only 8 orders of magnitude lower than η_{DL}. Even if in the bulk material with 1-cm length and $d_{\text{eff}}=43.9$ pm/V, the efficiency is only $\sim1.5\%$ at $I_{0FW}=50$ kW/cm^2. Figure 6 shows the dependence of I_{0FW} (required for achieving $\eta_{DL}=50\%$) on *PN*. I_{0FW} decreases exponentially with the increase of *PN*, because the field localized in the defect grows exponentially as increasing *PN*, see Fig. 4. Although the increase of *PN* can significantly fall the FW intensity, nevertheless the linewidth of the localized mode narrows rapidly (see Fig. 4). For the large *PN*, the linewidth of FW must be narrow enough; otherwise the most energy of the incident FW should be cut off and then lead to the sharp decrease of efficiency. Therefore, we must choose the appropriate number of PN to give attention to the suitable linewidth and the incident FW intensity. For $PN=7$, $\Delta\lambda_{FW}$ is ~0.09 nm (a coherent length of ~12.6 mm) that is very easily obtained from many commercial lasers. For $I_{0FW}=50$ kW/cm^2 required for achieving the efficiency of 50%, if a beam is focused to a 40-μm spot in diameter, correspondingly the required total FW power is

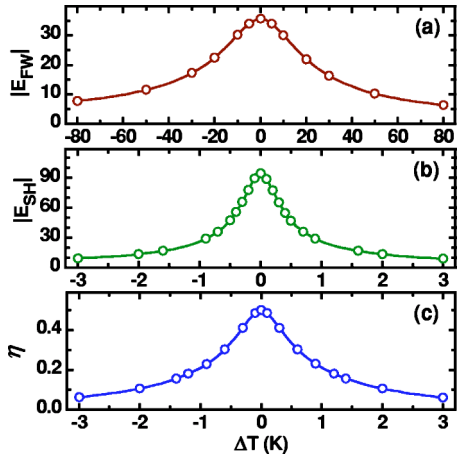

FIG. 7. (Color online) Dependence of $|E_{FW}|_{max}$, $|E_{SH}|_{max}$, and η on ΔT.

only ~600 mW, such low power can be generated even if from the continuous-wave lasers. Therefore, the dual-localization defective PC should be a promising nonlinear photonic device for performing the SHG of low power continuous-wave laser. If such a defective PC is integrated with the near IR laser diode (for instance, 890 nm), we can construct a compact and high-efficiency blue emitting device. However, for the defective PC's based on single localization[12] and the perfect PC's using band edge effect,[7] to obtain the efficiency of 50%, the required value of $I_{0\mathrm{FW}}$ is at least a few $\mathrm{MW/cm^2}$ even $\mathrm{GW/cm^2}$ order of magnitude. We also find such a feature that, in principle, the conversion efficiency in the defective PC's based on the localization character cannot achieve 100% because such a kind of SHG is not the perfect phase matching. A deviation of any one parameter from its designed value will change the performance of a device. As an example, we discuss the temperature effect, because the refractive index of the N layers ($LiNbO_3$) is temperature dependent. It can be found from Fig. 7 that the temperature deviation ΔT with respect to the designed temperature results in the rapid decrease of enhancement of FW and SH fields ($|E_{\mathrm{FW}}|$ and $|E_{\mathrm{SH}}|$) within the defect layer and the conversion efficiency η. The temperature band width of 46.0 K for $|E_{\mathrm{FW}}|$ is obviously broader than that of 1.0 K for $|E_{\mathrm{SH}}|$, which is agreement with the narrower spectral width $\Delta\lambda_{\mathrm{SH}}$ shown in Fig. 4. The temperature band width of η is 1.8 K having the same order as that of $|E_{\mathrm{SH}}|$, because which mostly depends on the narrowest one among $|E_{\mathrm{FW}}|$ and $|E_{\mathrm{SH}}|$.

In summary, we suggest a single defective PC with the dual-localized modes to realize the giant enhancement of second harmonic generation, analyze the features of localized modes based on the equivalent F-P cavity concept, and calculate the conversion efficiency by using the shooting method. Due to the salient features of high efficiency and low power density, such dual-localization defective PC's can be expected as a compact and high-efficiency nonlinear frequency-conversion photonic devices.

The authors acknowledge the support of NSFC Grants No. 90101030 and 10325417 ("Excellent Youth Foundation").

*Electronic address: htwang@nju.edu.cn

[1] E. Yablonovitch, Phys. Rev. Lett. **58**, 2059 (1987).
[2] S. John, Phys. Rev. Lett. **58**, 2486 (1987).
[3] M. Scalora, M. J. Bloemer, A. S. Manka, J. P. Dowling, C. M. Bowden, R. Viswanathan, and J. W. Haus, Phys. Rev. A **56**, 3166 (1997).
[4] V. Berger, Phys. Rev. Lett. **81**, 4136 (1998).
[5] M. Centini, C. Sibilia, M. Scalora, G. D'Aguanno, M. Bertolotti, M. J. Bloemer, C. M. Bowden, and I. Nefedov, Phys. Rev. E **60**, 4891 (1999).
[6] C. De Angelis, F. Gringoli, M. Midrio, D. Modotto, J. S. Aitchison, and G. F. Nalesso, J. Opt. Soc. Am. B **18**, 348 (2001).
[7] G. D'Aguanno, M. Centini, M. Scalora, C. Sibilia, Y. Dumeige, P. Vidakovic, J. A. Levenson, M. J. Bloemer, C. M. Bowden, J. W. Haus, and M. Bertolotti, Phys. Rev. E **64**, 016609 (2001).
[8] D. Pezzetta, C. Sibilia, M. Bertolotti, R. Ramponi, R. Osellame, M. Marangoni, J. W. Haus, M. Scalora, M. J. Bloemer, and C. M. Bowden, J. Opt. Soc. Am. B **19**, 2102 (2002).
[9] G. D'Aguanno, M. Centini, M. Scalora, C. Sibilia, M. Bertolotti, M. J. Bloemer, and C. M. Bowden, J. Opt. Soc. Am. B **19**, 2111 (2002).
[10] J. Martorell and R. Corbalan, Opt. Commun. **108**, 319 (1994).
[11] J. Trull, R. Vilaseca, J. Martorell, and R. Corbalan, Opt. Lett. **20**, 1746 (1995).
[12] B. Shi, Z. M. Jiang, and X. Wang, Opt. Lett. **26**, 1194 (2001).
[13] T. V. Dolgova, A. I. Maidykovski, M. G. Martemyanov, A. A. Fedyanin, O. A. Aktsipetrov, G. Marowsky, V. A. Yakovlev, G. Mattei, N. Ohta, and S. Nakabayashi, J. Opt. Soc. Am. B **19**, 2129 (2002).
[14] M. Soljačić and J. D. Joannopoulos, Nat. Mater. **3**, 211 (2004).
[15] Y. H. Ma, Opt. Quantum Electron. **15**, 529 (1983).
[16] D. H. Jundt, Opt. Lett. **22**, 1553 (1997).
[17] M. Born and E. Wolf, *Principles of Optics*, 6th ed. (Cambridge University Press, Cambridge, UK, 1998), p. 327.
[18] M. Born and E. Wolf, *Principles of Optics* (Ref. 17), p. 66.